

N92-14358

SEAL-ROTOR DYNAMIC-COEFFICIENT TEST RESULTS FOR A MODEL SSME ATD-HPFTP
TURBINE INTERSTAGE SEAL WITH AND WITHOUT A SWIRL BRAKE*

Dara W. Childs and Christopher Ramsey
Turbomachinery Laboratory
Mechanical Engineering Department
Texas A&M University
College Station, Texas 77843-3123, U.S.A.

Test results are presented and compared to theory for a model Space Shuttle Main Engine(SSME) Alternate Turbopump Development(ATD) High-Pressure Fuel Turbopump (HPFTP) with and without swirl brakes. Tests are conducted with supply pressures out to 18.3 bars and speeds out to 16,000 rpm. Seal back pressure is controlled to provide four pressure ratios at all supply pressures. Three inlet guide vanes are used to provide the following three fluid prerotation cases: (a) no prerotation, (b) moderate prerotation in the direction of rotation, and (c) high prerotation in the direction of rotation. Test results demonstrate the pronounced favorable influence of the swirl brake in reducing the seal destabilizing forces. Without the swirl brake, the cross-coupled stiffness k increases monotonically with increasing inlet tangential velocity. With the swirl brake, k tends to either be constant or decrease with increasing inlet tangential velocity. Direct damping either increases or remains relatively constant when the swirl brake is introduced. Direct stiffness is relatively unchanged. No measurable differences in leakage were detected for the seal with and without the swirl brake.

Comparisons between Scharrer's(1988) theory and measurements for the seal without a swirl brake indicate that the predictions can be used to provide design guidelines only. Specific predictions for rotordynamic coefficients should be treated cautiously, since systematic differences were observed between theory and experiment due to changes in running speed, supply pressure, and pressure ratio.

*The work reported herein was supported by NASA Lewis Research Center under contract NAG3-181; contract technical monitor: Robert Hendricks.

NOMENCLATURE

C, c	Direct and cross-coupled damping coefficients (FT/L)
K, k	Direct and cross-coupled stiffness coefficients (F/L)
\bar{K}, \bar{k}	Nondimensional direct and cross-coupled stiffness coefficients (dimensionless)
$f = k/C\omega$	Whirl frequency ratio (dimensionless)
L	Axial seal length (L)
Pra	Pressure ratio = discharge pressure/supply pressure
R_s	Seal-tip radius (L)
X, Y	Rotor to stator relative displacement components
$u_{\theta 0} = U_{\theta 0}/R_s \omega$	Nondimensional inlet tangential velocity
$U_{\theta 0}$	Inlet tangential velocity (L/T)
ω	Shaft angular velocity ($1/T$)

INTRODUCTION

Background and Motivation

For small motion about a centered position, the motion/reaction-force model for an annular gas seal is

$$-\begin{Bmatrix} F_X \\ F_Y \end{Bmatrix} = \begin{bmatrix} K & k \\ -k & K \end{bmatrix} \begin{Bmatrix} X \\ Y \end{Bmatrix} + \begin{bmatrix} C & c \\ -c & C \end{bmatrix} \begin{Bmatrix} \dot{X} \\ \dot{Y} \end{Bmatrix} \quad (1)$$

where X, Y are components of the rotor displacement vector relative to the housing, and F_X, F_Y are components of the reaction vector acting on the rotor. Further, K, k, C, c , are denoted as the direct stiffness, cross-coupled stiffness, direct damping, and cross-coupled damping coefficients, respectively. If one assumes a circular orbit of the seal at amplitude A and precessional frequency ω , the radial and tangential force coefficients can be stated

$$-F_r/A = K + c\omega \quad F_\theta/A = k - C\omega \quad (2)$$

Hence, K and c act in the radial direction and would be expected to predominantly influence rotor critical speeds, and k and c act in the tangential direction and would be expected to predominantly influence rotor stability. For a typical gas labyrinth seal, K and c have a negligible influence on rotordynamics; however, k can significantly degrade stability, while C can significantly improve stability. The cross-coupled stiffness coefficient k arises due to fluid rotation within the seal, and Wachter and Benchert(1980) demonstrated that a "swirl brake" consisting of radial ribs upstream of the seal, which reduce the inlet tangential velocity, could substantially reduce or eliminate k .

Pratt and Whitney(P&W) is in the process of developing an Alternate Turbopump Development(ATD) version of the SSME high pressure Turbopumps. The guidelines for their design requires direct interchangeability with the current Rock-etyne turbopumps and emphasizes reliability, reusability, and reduced manufacturing and maintenance costs. The units are nominally similar to the current designs; e.g., the ATD-HPFTP uses a three stage fuel pump driven by a two-stage turbine. However, various details related to rotordynamics are quite different. For example, the ATD-HPFTP has a high pressure drop across the turbine interstage seal; whereas, the current HPFTP does not. Because of the high-pressure drop, the rotordynamic coefficients increase sharply, and rotordynamics analysis of the ATD-HPFTP indicated a strong sensitivity of rotordynamic stability to the turbine interstage seal. Further analysis strongly suggested that a swirl brake be provided to reduce or eliminate the destabilizing forces developed by this seal.

The present test program compares predictions(Scharrer, 1988) and measurements for a model version of the seal, with and without a swirl brake, to establish a degree of confidence in seal calculations for the ATD turbopumps. Results are presented to answer the following questions:

- (a) How effective is the swirl brake in improving the stability characteristics of the seal, and
- (b) How good is Scharrer's theory in predicting rotordynamic coefficients?

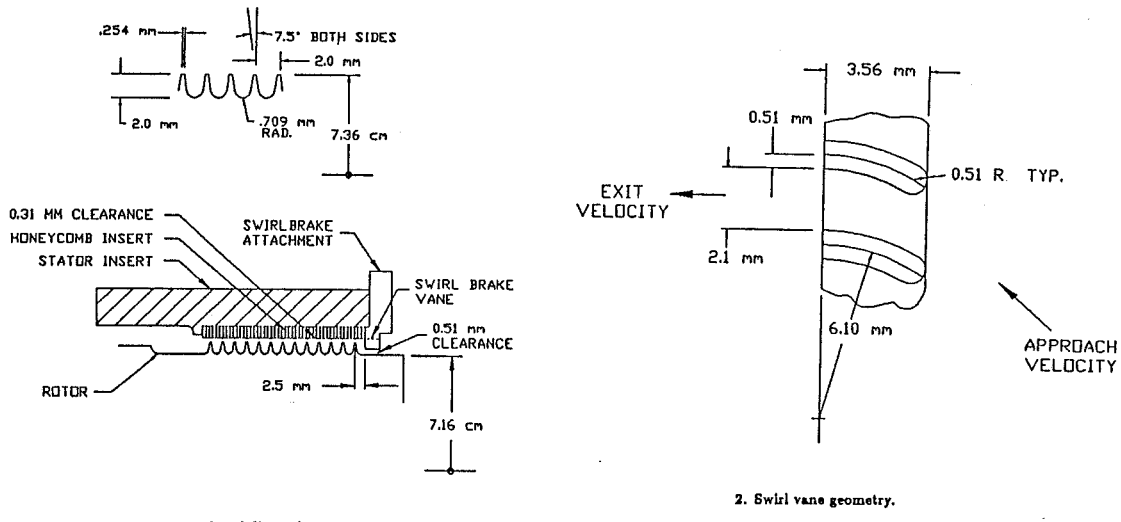
Test Hardware

As noted above, tests were undertaken for a model ATD-HPFTP turbine interstage seal which differs in the following details from the actual seal design:

- (a) The radius is smaller. The model seal has a labyrinth tip diameter of about 14.3cm versus the actual dimensions of about 20.2cm. This change was required by constraints of the test apparatus.
- (b) The test seal has twelve cavities versus five for the turbopump seal. This change was required to increase the measured force levels in the test apparatus, since the pressure drop across the seal is much lower in the test apparatus than the turbopump.
- (c) Test clearances between the labyrinth teeth and the honeycomb stator coincide with cold, nonrotating, conditions but are looser than hot operation conditions for the turbopump.

The model seal is otherwise identical with the ATD design using the same nominal axial clearance between the first labyrinth tooth and the swirl brakes, the same swirl-vane, tooth, and honeycomb-stator geometries.

Figure 1 illustrates the model seal dimensions, and figure 2 illustrates the swirl brake geometry. There are 145 individual vanes with a pitch between vanes of 3.12mm at their base radius of 7.42cm . Each vane is 2.1mm deep. The directions of the air approaching and leaving the swirl vanes in figure 2 are not necessarily representative of the performance of either the model or the turbopump swirl brake. They are provided to illustrate the intended function of the vanes in eliminating the tangential velocity entering the seal.



1. Model seal dimensions.

2. Swirl vane geometry.

Test Apparatus

The basic configuration of the test apparatus has been discussed in several earlier publications (Childs et al., 1986, Childs and Scharrer, 1988, etc.). Childs et al. (1990) have recently provided a discussion of modifications of the apparatus and facility involving: (a) the addition of a new compressor which increases the available supply pressure from 7.1 to 18 bars, (b) modification of the inlet preswirl arrangements, and (c) introduction of a swept-sine-wave excitation approach. With the original compressor, the full supply pressure was discharged across the test seal to obtain seal-amplitude forces which were large enough to measure. With the elevated supply pressure, the back pressure can be varied independently from the supply pressure and still yield measurable force amplitudes. Hence, the pressure ratio across the seal has been introduced as an independent parameter, and shorter seals can now be tested.

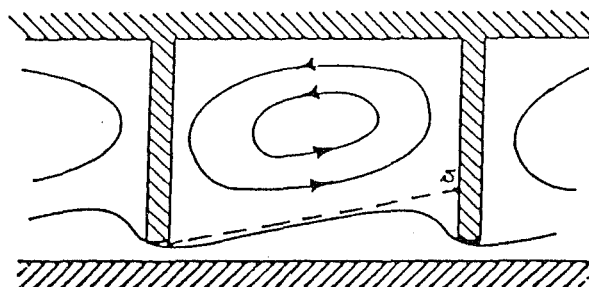
The basic apparatus is unchanged. The rotating seal is shaken horizontally by a hydraulic shaker, the reaction force components on the stator, due to relative seal motion, are measured and then corrected to account for stator acceleration, and the relative motion between the seal and stator are measured. From these measurements, the seal rotordynamic coefficients are calculated.

Scharrer's Theory(1988)

Scharrer uses a two-control-volume model to represent the known velocity distribution of a labyrinth seal illustrated in figure 3. The velocity field involves a through-flow leakage region next to the rotor and a vortex flow field in the labyrinth cavity. Scharrer's two-control-volume model has one control volume from the labyrinth tip to the stator and the second control volume in the labyrinth cavity. A free jet is assumed to exist between the two control volumes. The model for the seal involves the following equations:

- (a) an empirical leakage equation,
- (b) circumferential-momentum equations for both control volumes, and
- (c) continuity equations for the two control volumes.

The circumferential momentum equation for flow in the cavity includes the shear stresses at the solid boundary and a jet shear stress between the vortex flow and the through flow. Hirs(1973) turbulence model is used to define the sheer stresses between solid boundaries and the fluid.



3. Labyrinth-seal flow field.

Comparisons between Scharrer's theory and test results have been presented previously by Childs and Scharrer(1988) for teeth-on-stator(smooth-rotor) and teeth-on-rotor (smooth-stator) seals and by Hawkins and Childs(1988) for teeth-on-rotor seals with honeycomb stators. These results were for 5.08 cm long seals with the original 7.1 bar supply pressures at three clearances and showed generally reasonable agreement between theory and experiments.

EXPERIMENTAL RESULTS

Introduction

The test apparatus and facility used for this study were developed as part of an extended, joint NASA-USAF funded research program for annular gas seal studies.

The test fluid is air. As noted in the preceding section, the test apparatus provides an excitation about the centered position and has been thoroughly discussed in earlier publications.

Test Variables

When shaking about the centered position, the dynamic-seal apparatus is capable of controlling the following four independent variables: *supply pressure*, *pressure ratio*, *rotor speed*, and *inlet circumferential velocity*. The pressure ratio used here is discharge pressure divided by supply pressure; hence $Pra = 1$ implies no pressure difference, and $Pra \cong 0$ implies an infinite supply pressure. Test points for these independent variables are shown in table 1. Reference to the symbols of table 1 is helpful and necessary to understand the figures which follow.

The reservoir pressures, as measured upstream of the flowmeter, are given in table 1. These values differ (slightly) from the actual inlet pressure because of frictional losses and acceleration of the fluid due to inlet guide vanes. Tests are not run at zero pressure difference, since a small pressure difference is necessary to keep the rotor from shifting axially and rubbing the inlet-guide-vane assembly. No zero-rotor-speed tests were run, since rotor rotation is necessary to prevent damage to the thrust bearing during shaking.

Table 1. Definition of symbols used in figures.

Supply Pressures	Pressure Ratios	Rotor Speeds	Inlet Circumferential Velocities
1 - 7.9 bar	1 - .50	1 - 5000 cpm	0 - Zero tangential velocity
2 - 13.1 bar	2 - .42	2 - 12000 cpm	1 - Intermediate velocity with rotation
3 - 18.3 bar	3 - .35 4 - .30	3 - 16000 cpm	2 - High velocity with rotation

There were three test points for inlet circumferential velocity: one zero pre-rotation and two prerotated in the direction of shaft rotation. The zero-prerotation case is obtained with straightening vanes. The two different magnitudes of positive inlet circumferential velocity correspond to different inlet-guide-vane geometry depths. The calculated inlet tangential velocity tends to decrease with rotor speed, because the rotor grows with increased speed and reduces the leakage. The ratio of inlet circumferential velocity to rotor surface velocity ranges from zero to about 0.8.

Measurement of leakage flowrates showed no differences with and without the swirl brake.

Relative Uncertainty

The uncertainty in the dynamic coefficients can be determined using the method described by Holman(1978). The uncertainty in the force, excitation frequency, and displacement measurements are 0.55 N (0.125 lb), 0.065 Hz, and 0.0013 mm (0.05 mils), respectively. Before normalization, the nominal calculated uncertainty in the stiffness coefficients is 6.7 N/mm (38 lb/in) and 0.014 N-s/mm (0.082 lb-s/in) for the damping coefficients. The predicted uncertainties are generally satisfactory in comparison to nominal values for K and k . They are generally unsatisfactory for c and are only satisfactory for C at the highest supply pressure. Hence, data are presented for K and k at all test conditions, for C at the highest supply pressure, and are not presented for c .

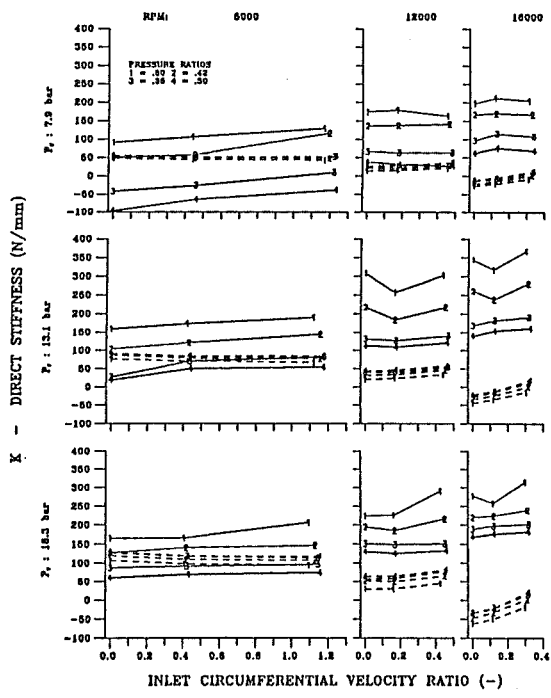
The principal source of uncertainty in the resultant force measurement is the acceleration measurement for the stator, not the piezo-electric force transducer measurements. The accelerometers used for these tests have a resolution of 5×10^{-3} g's. Although more sensitive accelerometers are available, they can not generally be used when testing honeycomb seals, because high-frequency accelerometer "spikes" are frequently seen with these seals, presumably because of a Helmholtz-acoustic excitation of the honeycomb cavities.

Test Results

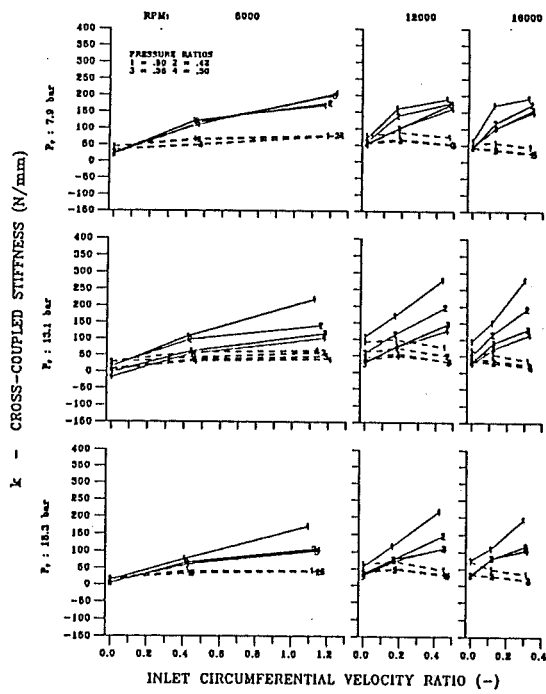
Figure 4 illustrates experimental and theoretical values for K versus $u_{\theta 0}$ for three speeds, three supply pressures, and four pressure ratios. The experimental results presented are for no swirl brake; however, very similar results were obtained with the swirl brake. Solid lines denote test results; dashed lines denote theoretical predictions. The theory does an adequate job of predicting K at low speeds; however, as the speed increases, K is progressively under predicted. The test results are much more sensitive to changes in the pressure ratio than the theory. Moreover, the theory predicts that K increases as Pra decreases, while tests show an opposite trend. The changes in K due to changes in speed are primarily due to changes in clearances. Nondimensionalization, which eliminates the influence of clearance, eliminates the apparent speed dependency.

Figure 5 illustrates k versus $u_{\theta 0}$ for the seal with and without swirl brakes. For the seal without the swirl brake, $u_{\theta 0}$ is the actual(calculated) normalized tangential velocity entering the seal. With the swirl brake, $u_{\theta 0}$ is the normalized tangential velocity entering the swirl brake. Obviously, the swirl brake sharply reduces k . At low speeds, k 's rate of increase with increasing $u_{\theta 0}$ is decreased. At higher speeds, k actually decreases as $u_{\theta 0}$ increases.

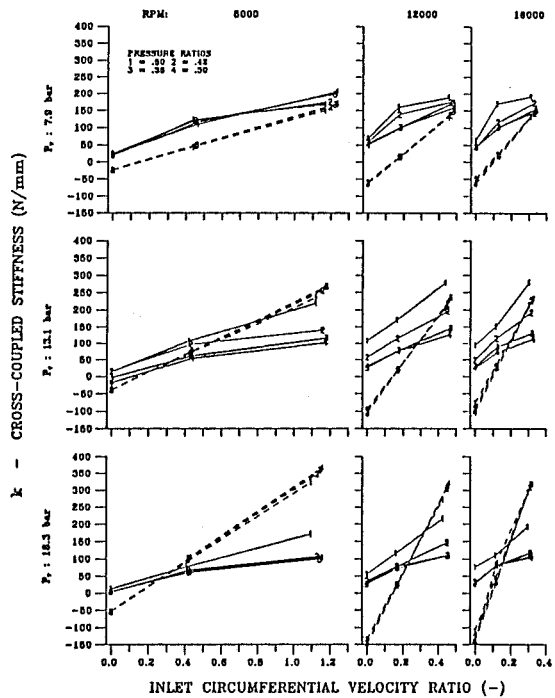
Figure 6 compares theory versus experiment for k for the seal without the swirlbrake. The theory does an adequate job at low speeds and low pressures but does poorly as the supply pressure and speed increase. Generally speaking,



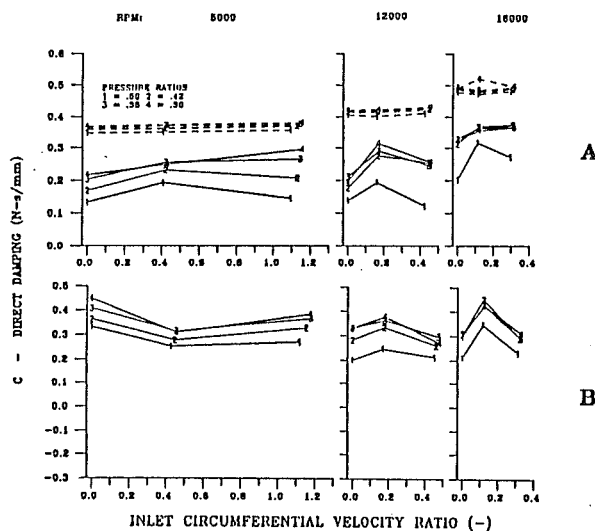
4. K versus $u_{\theta 0}$ for the seal without the swirl brake, for three speeds, three supply pressures, and four pressure ratios. Solid lines denote test data; dashed lines denote theory.



5. K versus $u_{\theta 0}$ for the seal with and without swirl brakes for three speeds, three supply pressures, and four pressure ratios. Dashed lines denote the seal with a swirl brake, solid lines without.



6. K versus $u_{\theta 0}$ for the seal without a swirl brake. Dashed lines represent the theory; solid lines represent test results.



7. Theory versus experimental results for C ; $P_r = 18.3$ bars:
(A) Theory versus experiment for the seal without a swirl brake,
(B) Experimental results with a swirl brake.

for low $u_{\theta 0}$, k is underpredicted, and measured k values increase more slowly than theoretical predictions as $u_{\theta 0}$ is increased. Measured results are much more sensitive to changes in the pressure ratio than predictions.

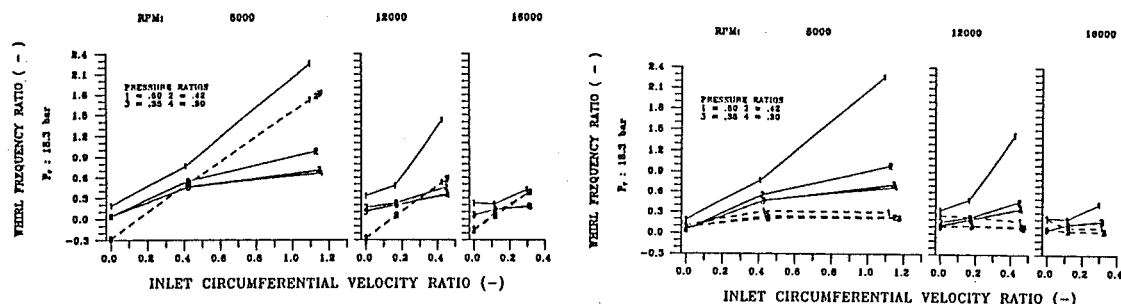
Figure 7 illustrates C versus $u_{\theta 0}$. The A frame of this figure provides theory versus experiment comparisons for the seal without the swirl brake. The B frame provides experimental results for the seal with the swirl brake. C is seen to be comparatively insensitive to changes in $u_{\theta 0}$. In A, the theory is seen to substantially overpredict C . Also, measured values of C are more sensitive to changes in Pra than theoretical predictions. Comparing the experimental results in A and B illustrates that the swirl brake increases C substantially at low speeds but has only a minimal influence at higher speeds. As noted earlier, test results are only presented for C at the highest supply pressure because of problems with excessive uncertainties at lower supply pressures.

A convenient overall measure of seal stability is the whirl-frequency ratio which is a nondimensionalized ratio of the destabilizing tangential force due to k and the stabilizing forces due to C . From equation(2), the definition is

$$f = k/C\omega$$

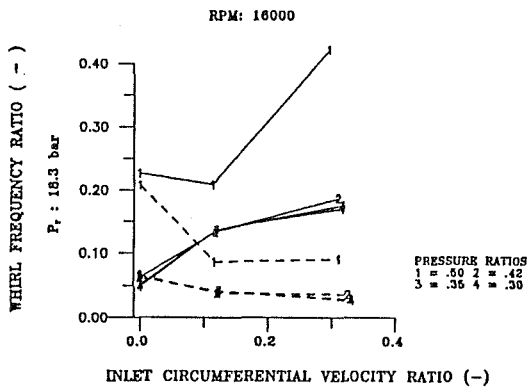
where ω is the shaft speed. Figure 8 illustrates f versus $u_{\theta 0}$. Theory versus experimental results are presented for the seal with no swirl brake. Measured results are much more sensitive to changes in the pressure ratio than predictions. Typically, f is underpredicted at low values for $u_{\theta 0}$, and measured values for f increase more slowly with increasing $u_{\theta 0}$ than predicted. For the results available, correlation between theory and experiment improve as running speed increases.

Figure 9 compares f versus $u_{\theta 0}$ results with and without the swirl brake. Obviously, the swirl brake sharply reduces f and sharply increases stability of the seal. The scaling used in this figure suggests that the swirl brake is becoming less effective as speed increases; however, figure 10 shows that the swirl brake is exceptionally effective at the highest speed. With the swirl brake, f decreases with increasing $u_{\theta 0}$ and is much lower.



8. Theory and experimental results for f versus $u_{\theta 0}$, no swirl brake; $P_r = 18.3$ bars.

9. f versus $u_{\theta 0}$ with and without a swirl brake; $P_r = 18.3$ bars.



10. f versus $u_{\theta 0}$ with and without a swirl brake; $\omega = 16,000 \text{ rpm}$; $P_r = 18.3 \text{ bars}$.

Discussion

The outstanding effectiveness of the swirl brake in reducing destabilizing forces developed by the seal largely speaks for itself. The present results echo those of a companion paper, Childs et al.(1990), in emphasizing the advantages accruing to an aerodynamically designed swirl brake.

As noted earlier, Scharrer's(1988) theory uses Hirs(1973) results to model the wall shear stresses on the fluid. Hirs' model defines the stress on the fluid at a wall in terms of the friction-factor definition

$$\lambda = nR^m$$

where the Reynolds number R is defined in terms of the average bulk-flow velocity relative to the wall. The empirical parameters n, m characterize wall roughness. The present theoretical predictions used

$$nr = 0.079, \quad mr = -0.25 \quad (3)$$

for the smooth rotor, and

$$ns = 0.047, \quad ms = -0.1275 \quad (4)$$

for the honeycomb stator surfaces. The results of equation (3) were developed by Yamada(1962) from measurements of flow between rotating cylinders. The results of equation(4) are from Ha(1989) and are based on flat-plate test results for the honeycomb cell dimensions used in this study. When friction factors based on the coefficients of equation(4) are plotted on a Moody diagram, the equivalent relative roughness parameter is about 0.03. When the friction factor was increased(arbitrarily) by about a factor of twenty, much better agreement between theory and measurements were obtained. The authors have no explanation for this

result and do not endorse this sort of arbitrary manipulation of the model; however, the results suggest that higher energy dissipation is present in the seal than accounted for by Scharrer's(1988) model. Since the empirical model used for leakage predictions does not account for a deliberately roughened stator, no comparisons are presented between theory and experiment for leakage.

SUMMARY AND CONCLUSIONS

Swirl-Brake Effectiveness

The aerodynamically-designed swirl brake proposed for the ATD-HPFTP turbine interstage seal is remarkably effective. It reduces k markedly and actually yields a reduction in k with increasing values for $u_{\theta 0}$.

Theory versus Experiment

A summary review of theory versus experiment for the rotordynamic coefficients and the whirl frequency ratio follows:

- K*: The theory does a good job at low speeds; however, as the speed increases, K is substantially underpredicted. As the speed is increased, increasing supply pressure magnifies this difference between theory and experiment. Measured values of K are more sensitive to changes in Pra than predicted. Also, in contrast to predictions, measured K values increase with increasing Pra .
- k*: The theory does a good job at low speeds and low supply pressures. Increases in either the speed or supply pressure degrades agreement between theory and prediction. Typically, k is underpredicted for zero $u_{\theta 0}$ and increases more slowly than predicted. Also, k is much more sensitive to changes in Pra than predicted.
- C*: The theory underpredicts C , but the correlation improves(slightly) as speed is increased. Measured results are more sensitive to changes in Pra than predicted.
- $f = k/Cw$: The theory does a reasonable job, and the comparison between theory and experiment improves as speed is increased. Measured f values are higher than predicted at low values of $u_{\theta 0}$. A reasonable prediction of f results from compensating errors in predicting C (too high) and k (too low) for higher values of $u_{\theta 0}$.

Conclusions

The results presented here support the following general conclusions:

- (a) The proposed swirl brake design is remarkably effective.
- (b) Scharrer's(1988) theory can provide some basic guidance for the analysis of tooth-on-rotor/honeycomb stator annular seals; however, discrepancies between theory and measurements can be pronounced. An improved theoretical model for this type of seal is clearly needed.

REFERENCES

- Benchert, H., and Wachter, J.(1980), "Flow Induced Spring Coefficients of Labyrinth Seals for Application in Rotordynamics," NASA CP2133, Proceedings of the workshop: Rotordynamic Instability Problems in High Performance Turbomachinery, held at Texas A&M University, 12-14 May 1980, pp. 189-212.
- Childs, D. W., Baskharone, E. A., and Ramsey, C.(1990), "Test Results for Rotordynamic Coefficients of the SSME HPOTP Turbine Interstage Seal With Two Swirl Brakes," submitted for review *ASME Journal of Tribology*, Feb. 1990.
- Childs, D. W., and Scharrer, J.(1988), "Theory Versus Experiment for the Rotordynamic Coefficients of Labyrinth Gas Seals: Part II - A Comparison to Experiment," *ASME Journal of Vibration, Acoustics, Stress, and Reliability in Design*, Vol. 110, No. 3, July 1988, pp. 281-287.
- Childs, D. W., Nelson, C. E., Nicks, C., Scharrer, J., Elrod, D., and Hale, K.(1986), "Theory Versus Experiment for the Rotordynamic Coefficients of Annular Gas Seals: Part 1-Test Facility and Apparatus," *ASME Transaction Journal of Tribology*, Vol. 108, pp. 426-432.
- Ha, T. W.(1989), "Friction Factor Data for Flat-Plate Tests of Smooth and Honeycomb Surfaces," TL-SEAL-1-89, Turbomachinery Laboratory Report, Texas A&M University, May 1989.
- Hawkins, L., Childs, D., and Hale, K.(1988), "Experimental Results for Labyrinth Gas Seals With Honeycomb Stators: Comparisons to Smooth Stator Seals and Theoretical Predictions," *ASME Journal of Tribology*, Vol. 111, No. 1, pp. 161-168, Jan. 1989.
- Hirs, G. G.(1973), "A Bulk-Flow Theory for Turbulence in Lubricant Films," *ASME Journal of Lubrication Technology*, April 1973, pp. 137-146.
- Holman, J. P.(1978), *Experimental Methods for Engineers*, McGraw Hill, 1978, pp. 45.
- Scharrer, J.(1988), "Theory Versus Experiment for the Rotordynamic Coefficients of Labyrinth Gas Seals: Part I - A Two Control Volume Model," *ASME Journal of Vibration, Acoustics, Stress, and Reliability in Design*, Vol. 110, No. 3, July 1988, pp. 270-280.
- Yamada, Y.(1962), "Resistance of Flow Through an Annulus with an Inner Rotating Cylinder," *Bull. JSME*, Vol.5, No. 18, 1962, pp. 302-310.